J|A|C|S ARTICLES

Published on Web 06/03/2010

Enantioselective Separation on Chiral Au Nanoparticles

Nisha Shukla,[†,‡] Melissa A. Bartel,[†] and Andrew J. Gellman*[,†,‡]

Institute of Complex Engineered Systems and Department of Chemical Engineering, Carnegie Mellon University, Pittsburgh, Pennsylvania 15213, and National Energy Technology Laboratory, U.S. Department of Energy, P.O. Box 10940, Pittsburgh, Pennsylvania 15236

Received September 27, 2009; E-mail: gellman@cmu.edu

Abstract: The surfaces of chemically synthesized Au nanoparticles have been modified with D- or L-cysteine to render them chiral and enantioselective for adsorption of chiral molecules. Their enantioselective interaction with chiral compounds has been probed by optical rotation measurements during exposure to enantiomerically pure and racemic propylene oxide. The ability of optical rotation to detect enantiospecific adsorption arises from the fact that the specific rotation of polarized light by (*R*)- and (*S*)-propylene oxide is enhanced by interaction with Au nanoparticles. This effect is related to previous observations of enhanced circular dichroism by Au nanoparticles modified by chiral adsorbates. More importantly, chiral Au nanoparticles modified with either D- or L-cysteine selectively adsorb one enantiomer of propylene oxide from a solution of racemic propylene oxide, thus leaving an enantiomeric excess in the solution phase. Au nanoparticles modified with L-cysteine (D-cysteine) selectively adsorb the (*R*)-propylene oxide ((*S*)-propylene oxide). A simple model has been developed that allows extraction of the enantiospecific equilibrium constants for (*R*)- and (*S*)-propylene oxide adsorption on the chiral Au nanoparticles.

Introduction

Considerable effort has been expended over the past decade on the synthesis of metallic nanoparticles with controlled size, shape, composition, and morphology. In the field of catalysis, much of the effort is motivated by the desire to control catalytic selectivity by controlling nanoparticle shape and structure such that the catalytic surface exposes a homogeneous set of active sites for reaction.[1] The logic is that catalysts with active sites all having the same local structure will have the highest achievable selectivity for a given chemical process. Among all forms of catalytic selectivity, enantioselectivity is perhaps the most subtle and the most difficult to control. To this end, the controlled synthesis of enantiomerically pure chiral metal nanoparticles could serve as a new route to enantioselective catalytic materials. Over the past decade, there has been considerable interest and effort devoted to the synthesis and characterization of chiral, optically active metal nanoparticles capped with chiral organic ligands.[2−4] In this work, we use wet chemical synthesis methods to prepare chiral Au nanoparticles and then use polarimetry to show that these chiral nanoparticles are capable of enantioselective adsorption of chiral compounds. The fact that these chiral nanoparticles interact enantiospecifically with chiral adsorbates is a key step toward achieving enantiospecific catalysis, separations, and sensing.

The bulk of existing work on chiral Au nanoparticles has focused on structure determination and understanding of the origin of their optical activity. The absolute structure determination of a Au_{102} cluster coated with 44 *p*-mercaptobenzoic acid ligands revealed that it is chiral.[5] Although the core of the Au cluster is symmetric, the outer layer of Au atoms coordinated to the *p*-mercaptobenzoic acid has a chiral structure. The structures of two smaller Au_{25} clusters have been determined using XRD and NMR and shown to be identical and achiral.[6,7] The first studies of the optical activity of Au nanoparticles (20−40 atoms) modified by chiral ligands (glutathione) showed that they exhibit strong optical activity as observed using circular dichroism.[8] Since then, a significant level of effort has been expended on the determination of the origins of this optical activity in either the Au core or the chiral ligand layer.[2−4,9,10] Other ligands used to prepare Au nanoparticles modified by chiral adsorbates include: 2,2′-bis(diphenylphosphino)-1,1′-binaphthyl,[11] *N*-iosbutyry-L-cysteine,[12,13] and penicillamines.[14]

In addition to optical activity, such chiral Au nanoparticles should exhibit enantiospecific interactions with chiral probe molecules, and it is these interactions that are the root of

[†] Carnegie Mellon University.
[‡] U.S. Department of Energy.

(1) Lee, I.; Delbecq, F.; Morales, R.; Albiter, M. A.; Zaera, F. *Nat. Mater.* **2009**, *8* (2), 132–138.
(2) Gautier, C.; Burgi, T. *ChemPhysChem* **2009**, *10* (3), 483–492.
(3) Noguez, C.; Garzon, I. L. *Chem. Soc. Rev.* **2009**, *38* (3), 757–771.
(4) Yao, H. *Current Nanosci.* **2008**, *4* (1), 92–97.
(5) Jadzinsky, P. D.; Calero, G.; Ackerson, C. J.; Bushnell, D. A.; Kornberg, R. D. *Science* **2007**, *318* (5849), 430–433.
(6) Heaven, M. W.; Dass, A.; White, P. S.; Holt, K. M.; Murray, R. W. *J. Am. Chem. Soc.* **2008**, *130* (12), 3754.
(7) Wu, Z. W.; Gayathri, C.; Gil, R. R.; Jin, R. C. *J. Am. Chem. Soc.* **2009**, *131* (18), 6535–6542.
(8) Schaaff, T. G.; Whetten, R. L. *J. Phys. Chem. B* **2000**, *104* (12), 2630–2641.
(9) Canfield, B. K.; Kujala, S.; Laiho, K.; Jefimovs, K.; Vallius, T.; Turunen, J.; Kauranen, M. *J. Nonlinear Opt. Phys. Mater.* **2006**, *15* (1), 43–53.
(10) Hidalgo, F.; Sanchez-Castillo, A.; Garzon, I. L.; Noguez, C. *Eur. Phys. J. D* **2009**, *52* (1−3), 179–182.
(11) Tamura, M.; Fujihara, H. *J. Am. Chem. Soc.* **2003**, *125* (51), 15742–15743.
(12) Gautier, C.; Burgi, T. *J. Am. Chem. Soc.* **2008**, *130* (22), 7077–7084.
(13) Gautier, C.; Burgi, T. *J. Am. Chem. Soc.* **2006**, *128* (34), 11079–11087.
(14) Yao, H.; Miki, K.; Nishida, N.; Sasaki, A.; Kimura, K. *J. Am. Chem. Soc.* **2005**, *127* (44), 15536–15543.

enantioselective chemical processes, enantiospecific sensing, and other applications. These types of enantiospecific interactions between chiral adsorbates and chiral metal nanoparticles ought to be similar in nature to those observed on chiral surfaces.[15−17]

This paper describes the successful synthesis of chiral Au nanoparticles with surfaces modified by racemic cysteine or enantiomerically pure D- or L-cysteine. They have been selected for study because thiols, in general, are known to bind strongly to Au surfaces through deprotonation of the thiol group to form a thiolate. On single-crystal Au surfaces, cysteine has been show to adsorb by deprotonation of the thiol group to give a strongly bound thiolate which also interacts with the surface via the amine group.[18] Formation of a thiolate is also known to be the case for Au nanoparticles.[5] In this work, the enantiospecific adsorption of racemic propylene oxide (PO) and enantiomerically pure (*R*)- or (*S*)-PO onto these modified Au nanoparticles has been probed using polarimetry. PO has been chosen as a chiral titrant because it is not likely to react with the Au surfaces and there is prior evidence of its enantiospecific adsorption on naturally chiral Cu surfaces.[16] One interesting result of this work is that the specific rotation of polarized light by both PO and cysteine is enhanced by interaction with the Au nanoparticles. As a result, it is possible to use polarimetry as a simple means of differentiating between chiral molecules in solution and chiral molecules interacting with Au nanoparticles. This has allowed the more important observation, from the perspective of this work, of the enantioselective adsorption of (*R*)- and (*S*)-PO on Au nanoparticles that have been chirally modified with either D- or L-cysteine. When exposed to racemic mixtures of PO, the chiral Au nanoparticles selectively adsorb one enantiomer leaving an excess of the other enantiomer in solution, thereby inducing enantioselective separation.

Experimental Section

The procedure for the synthesis of Au nanoparticles was adapted from a procedure published by Jana et al.[19] Two different methods were used for coating the Au nanoparticles with cysteine: exposing the Au nanoparticles to cysteine 24 h after their synthesis and exposing the Au nanoparticle to cysteine during their synthesis. Three types of cysteine coatings were used for the various experiments: D-cysteine, L-cysteine, and racemic cysteine. The Au nanoparticle solutions were stored overnight prior to optical rotation measurements. The properties of the Au nanoparticles were not sensitive to the method used to modify their surfaces with cysteine.

Cysteine Coating Following Au Nanoparticle Synthesis. A 20 mL aqueous solution of 2.5×10^{-4} M Au chloride and 2.5×10^{-4} M sodium citrate was prepared in a round-bottom flask. Then, 0.6 mL of ice-cold 0.1 M sodium borohydride solution was added slowly. The solution was allowed to stir for 2 h at room temperature, until the solution changed from red to deep purple in color. The solution was stored overnight in a glass vial wrapped in aluminum foil to prevent light degradation. The Au nanoparticle solution was diluted (1 mL solution in 5 mL water), and cysteine was added to the diluted solution to a total concentration of 0.025 M. The solution was allowed to sonicate for 30 min prior to use.

Cysteine Coating during Au Nanoparticles Synthesis. A 15 mL aqueous solution of 3.33×10^{-4} M Au chloride and 3.33×10^{-4} M sodium citrate was prepared in a round-bottom flask. Then, 0.6 mL of ice-cold 0.1 M sodium borohydride solution was added slowly. Immediately following the addition of the sodium borohydride solution, 5 mL of 0.6 M cysteine was injected. The solution was allowed to stir for 2 h at room temperature, until the solution changed from red to deep purple in color. The solution was stored overnight in a glass vial wrapped in aluminum foil to prevent light degradation. The cysteine-coated Au nanoparticle solution was diluted (1 mL solution in 5 mL of water) prior to use. This yielded solutions with the same net concentrations of Au nanoparticles and cysteine as the method in which cysteine was added postsynthesis.

Au(III) chloride trihydrate (>99.9%), sodium citrate, sodium borohydride, L-cysteine (>97%), D-cysteine (99%), and *rac*-cysteine (>97%) were purchased from Sigma Aldrich and were used without purification. (*R*)- and (*S*)-propylene oxide were purchased from Alfa Aesar.

X-ray Diffraction. Samples were analyzed using a Panalytical X'Pert Pro X-ray diffractometer. The sample was prepared by evaporation of 0.5 mL of the colloidal Au nanoparticle solution onto a glass microscope slide.

Optical Rotation Measurements. Samples were analyzed using a Rudolph Research Analytics Autopol IV polarimeter at a wavelength of 436 nm, and all measurements were made at room temperature. The diluted cysteine-coated Au nanoparticle solutions described in the synthesis section were used to measure the optical rotation. The 6 mL solution was poured into a glass polarimeter tube with a filler cap, and the solution was placed inside the polarimeter for analysis. For measurements that required increments of propylene oxide to be added to the solution, the solution was poured into a small beaker, pure propylene oxide was added, and the solution was stirred using a glass stirrer and then poured back into the glass polarimeter tube. Addition of propylene oxide to a concentration of 1 M required the addition of 0.4 mL by volume to the 6 mL solution of Au nanoparticles. The solutions used for the optical rotation measurement contained only the PO (varying concentrations) and the Au nanoparticles (fixed concentration).

Results

The synthesis method described above yields Au nanoparticles suspended in aqueous solution. The surfaces of these nanoparticles can be modified with cysteine either during the synthesis or afterward by addition of cysteine to the solution. Under these conditions, it is expected that the cysteine should be adsorbed via deprotonation of the thiol group in order to form adsorbed thiolate.[5,18] TEM showed that the Au nanoparticles do not have a well-defined shape but are roughly oval with a fairly narrow size distribution having an average diameter of ∼5 nm. The overall shapes of these Au nanoparticles are not chiral. Thus, the enantioselectivity that these nanoparticles exhibit must arise from local interactions between chiral adsorbates ((*R*)- or (*S*)-PO) and the chirally modified (D- or L-cysteine) surfaces of the Au nanoparticles.

The enantioselective adsorption of PO onto cysteine-modified Au nanoparticles has been probed using polarimetry. Calibration of the polarimetry measurements using enantiomerically pure (*R*)- or (*S*)-PO in aqueous solution at concentrations up to 0.4 M is shown in Figure 1 with solid circles (●). The optical rotations are opposite and linear in the concentrations of (*R*)- or (*S*)-PO. The data indicate a specific rotation of 0.90 ± 0.06 °/M. Also plotted in Figure 1 are the optical rotations of (*R*)- or (*S*)-PO in solutions containing bare Au nanoparticles and Au nanoparticles modified by adding racemic cysteine (*rac*-cys/Au) to the solution at a concentration of 0.025 M. These Au nanoparticles have no net chirality, and so, they cannot interact enantiospecifically with either (*R*)- or (*S*)-PO. The rotation of polarized light resulting from the addition of (*R*)- or

(15) Horvath, J. D.; Baker, L.; Gellman, A. J. *J. Phys. Chem. C* **2008**, *112* (20), 7637–7643.
(16) Horvath, J. D.; Gellman, A. J. *J. Am. Chem. Soc.* **2001**, *123* (32), 7953–7954.
(17) McFadden, C. F.; Cremer, P. S.; Gellman, A. J. *Langmuir* **1996**, *12* (10), 2483–2487.
(18) Greber, T.; Sljivancanin, Z.; Schillinger, R.; Wider, J.; Hammer, B. *Phys. Rev. Lett.* **2006**, *96*, (5).
(19) Jana, N. R.; Gearheart, L.; Murphy, C. J. *J. Phys. Chem. B* **2001**, *105* (19), 4065–4067.

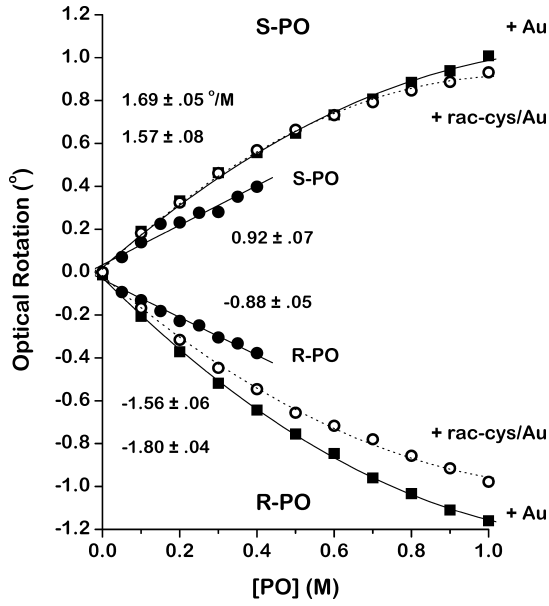

Figure 1. Rotation of light by enantiomerically pure (*R*)- and (*S*)-PO in various media. When dissolved in water (●), the (*R*)- and (*S*)-PO rotate light by equal and opposite angles with a specific rotation of 0.9°/M. In the presence of Au nanoparticles (■) and Au nanoparticles coated with racemic cysteine (○) (cysteine concentration of 0.025 M) the specific rotation is increased measurably.

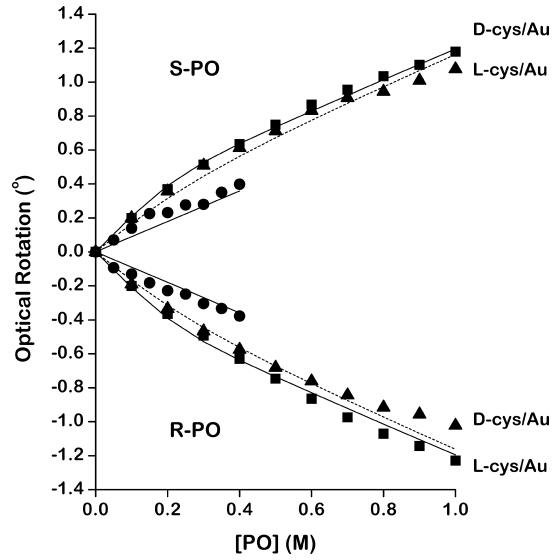

Figure 2. Optical rotation by (*R*)- and (*S*)-PO in pure aqueous solutions (●) and in solutions containing Au nanoparticles modified with D- and L-cysteine. The data from the solutions containing the heterochiral pairs ((*R*)-PO/L-cys and (*S*)-PO/D-cys) are marked with solid squares (■). The data from solutions containing the homochiral pairs ((*R*)-PO/D-cys and (*S*)-PO/L-cys) are marked with solid triangles (▲). The solid and dashed lines mark the fits of the adsorption model described in the text. The deviations between the data for the homochiral and the heterochiral pairs are indicative of the enantiospecific interaction of (*R*)- and (*S*)-PO with the chiral Au nanoparticles.

(*S*)-PO to the solutions of Au nanoparticles clearly deviates from the optical rotation of solutions containing just (*R*)- or (*S*)-PO. This indicates that there is some interaction between the PO and the Au nanoparticles in solution, presumably via adsorption of some PO onto the Au nanoparticles. The fact that the rotation of light by (*R*)- and (*S*)-PO is enhanced by the presence of the Au nanoparticles suggests that the specific rotation of light by PO is increased by adsorption onto the Au nanoparticles. This observation is consistent with reports of enhanced circular dichroism by Au nanoparticles modified with glutathione, a cysteine containing tripeptide (γ-glu-cys-glu).[8] Figure 1 shows that the rotation of light by (*R*)- or (*S*)-PO in the presence of Au nanoparticles varies nonlinearly with PO concentration. This is likely to be the result of adsorption described by an isotherm in which the adsorbed PO saturates the surfaces of the Au nanoparticles at some point within the concentration range covered by the measurements (<0.4 M). The fits to the optical rotations of (*R*)- and (*S*)-PO in the presence of Au nanoparticles are simply second-order polynomials which have been used to estimate their slopes at [PO] = 0. These indicate that the magnitudes of the optical rotations are 1.7 ± 0.1°/M, almost twice those of the pure (*R*)- and (*S*)-PO in solution. Note that these are not the specific optical rotations of adsorbed (*R*)- or (*S*)-PO because even at low total PO concentrations these solutions contain some fraction of PO in solution. The measured optical rotation of 1.7 ± 0.1°/M represents a lower limit on the specific optical rotation by (*R*)- or (*S*)-PO adsorbed on the Au nanoparticles. The important point, however, is that the enhanced optical rotation of light by (*R*)- or (*S*)-PO adsorbed on the Au nanoparticles allows differentiation of (*R*)- or (*S*)-PO in the adsorbed phase and the solution phase. Thus it serves as the basis for detection of enantiospecific interaction between (*R*)- or (*S*)-PO and Au nanoparticles that have been chirally modified with D- or L-cysteine.

In order to observe enantiospecific interactions between (*R*)- or (*S*)-PO and the chirally modified Au nanoparticles, optical rotation measurements have been made during exposure of D- or L-cysteine-modified Au nanoparticles to (*R*)- or (*S*)-PO (figure 2). Note that the Au nanoparticles modified by adsorbed D- or L-cysteine induce some intrinsic rotation of light at [PO] = 0. These values have been subtracted from the data in Figure 2 at all values of [PO]. For reference, the optical rotations by solutions containing just (*R*)- or (*S*)-PO at varying concentrations are shown again using solid circles (●). The enantiospecific interaction of the (*R*)- or (*S*)-PO with the chiral Au nanoparticles is apparent from the deviation between the data for the diastereomeric pairs of adsorbate ((*R*)- or (*S*)-PO) and modifier (D- or L-cysteine). The optical rotations by the (*R*)-PO/D-cys/Au and (*S*)-PO/L-cys/Au are indicated with solid squares (■) and are clearly greater in magnitude than those of (*S*)-PO/D-cys/Au and (*R*)-PO/L-cys/Au shown with the solid triangles (▲). Some systematic differences between the data sets for (*R*)-PO and (*S*)-PO are observable. These may arise from slight differences in laboratory temperature that influence the adsorption isotherms. The lines in Figure 2 are the fits of the entire data set to a fairly simple adsorption model described in the discussion section. Note that the magnitudes of the slopes at [PO] = 0, for the PO interacting with the Au nanoparticles are greater than those of pure PO, again revealing the enhanced rotation of light by PO adsorbed on Au nanoparticles.

In order to observe enantiospecific interactions between PO and chirally modified Au nanoparticles, optical rotation measurements have been made during addition of racemic PO (*rac*-PO) to solutions containing the chirally modified Au nanoparticles (Figure 3). Racemic PO has no net chirality and by itself does not induce any rotation of light. Addition of racemic PO to solutions containing chiral Au nanoparticles can only induce rotation of light, if there is an enantiospecific interaction between one enantiomer of the PO and the chiral Au nanoparticles resulting in a net excess of one enantiomer in the adsorbed state and the other in the solution phase. Detection of this partitioning

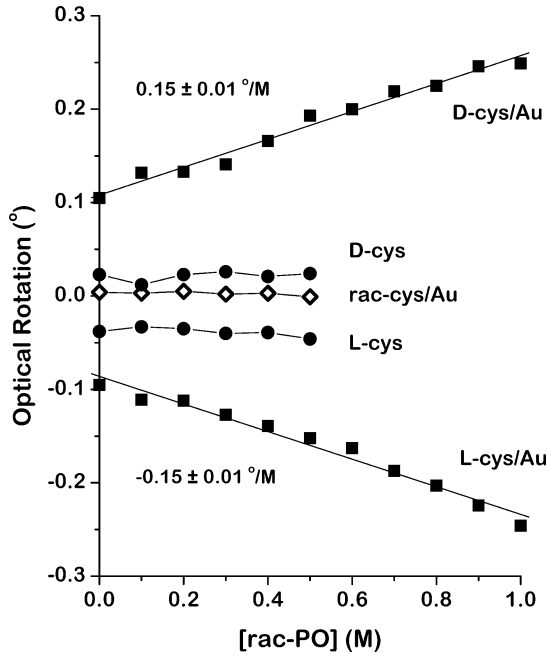

Figure 3. Rotation of polarized light by racemic PO added to solutions containing: Au nanoparticles modified with racemic cysteine (◊), L- or D-cysteine (●), and Au nanoparticles modified by L- or D-cysteine (■). The control measurements show that there are no enantiospecific interactions between PO and L-cysteine (●), D-cysteine (●), or Au nanoparticles coated with racemic cysteine (◊). PO does interact enantiospecifically with Au nanoparticles coated with either L- or D-cysteine (■), thus causing increased rotation of polarized light with increasing addition of racemic PO.

is only possible because the specific optical rotation constants in the adsorbed and solution phases differ.

Prior to making measurements of optical rotation using racemic PO, several control measurements have been made. First, Figure 3 shows the optical rotation observed during addition of *rac*-PO to a solution containing Au nanoparticles modified by racemic cysteine (*rac*-cys/Au) at a concentration of 0.025 M. Neither the PO nor the *rac*-cys/Au have any net chirality, and so, as expected, there is no net optical rotation during addition of the *rac*-PO to the solution. Second, rac-PO has been added to solutions containing enantiomerically pure D- or L-cysteine (0.025 M). The solutions containing pure D- or L-cysteine rotate polarized light; however, the addition of *rac*-PO does not change the degree of optical rotation. This is an important control experiment as it indicates that there are no detectable enantiospecific interactions between the PO and D- or L-cysteine in solution. Thus, any optical rotation observed during the addition of *rac*-PO to solutions containing Au nanoparticles modified by D- or L-cysteine cannot be attributed to interactions between PO and residual cysteine in the solution.

Au nanoparticles modified by D- or L-cysteine rotate polarized light, as indicated by the data in Figure 3 at [PO] = 0, the intercepts of the curves labeled D- or L-cys/Au (0.025 M). Note that the concentration of D- or L-cysteine in these solutions is the same as that used for the measurements of the rotational polarization of pure D- or L-cysteine in solution, and yet, the rotation of light in those solutions containing D- or L-cys/Au nanoparticles is ~4 times that of the solutions with just D- or L-cysteine. This is another example of the enhanced rotation of light by chiral molecules when adsorbed on Au nanoparticles.

The key result of this work is the observation that *rac*-PO interacts enantiospecifically with D- or L-cys/Au nanoparticles. The curves labeled D- or L-cys/Au in Figure 3 show that the addition of *rac*-PO to a solution containing D- or L-cys/Au nanoparticles results in increasing rotation of polarized light. If there were no enantiospecific interaction, then these curves would be flat, showing no change in optical rotation with addition of *rac*-PO to the solutions. The observed change in optical rotation resulting from the addition of *rac*-PO to solution is a rigorous indicator of the selective adsorption of one enantiomer of PO onto the surfaces of the Au nanoparticles leaving an excess of the other enantiomer of PO in solution. Given that we have already demonstrated the enhanced rotation of polarized light by PO adsorbed on the surfaces of the Au nanoparticles, the results in figure 3 suggest that (*S*)-PO adsorbs selectively on the surfaces of the D-cys/Au nanoparticles and that (*R*)-PO adsorbs selectively on the L-cys/Au nanoparticles. The net result is an enantioselective separation and enantiomeric purification of the PO remaining in solution.

Discussion

The data shown in Figures 2 and 3 indicate enantiospecific adsorption of *rac*-, (*R*)-, and (*S*)-PO onto Au nanoparticles modified with D- or L-cysteine. The data of Figure 2 can be classified by the direction or sign of the change in polarization (positive or negative) induced by changing the modifier from D- to L-cysteine for a given enantiomer of PO. The change in the direction of the polarization for (*S*)-PO when the modifier is switched from D- to L-cysteine is given by $X = (\theta^{S/D} - \theta^{S/L})/|\theta^{S/D} - \theta^{S/L}|$. The rotation angle for any given concentration of (*S*)-PO in a solution containing Au nanoparticles modified by D-cysteine is given by $\theta^{S/D}$. The sign of the change is opposite for (*R*)-PO; $X = (\theta^{R/L} - \theta^{R/D})/|\theta^{R/L} - \theta^{R/D}|$. The data set of Figure 2 constitutes $N = 20$ pairs of measurements of which 19 have $X = 1$ and one has $X = -1$, yielding a mean value of $\bar{X} = 0.9$. The data of Figure 3 are differential measurements of PO adsorption from racemic mixtures onto Au nanoparticles modified by D- or L-cysteine. Each of the differential measurements can be classified according to the sign of the rotation. For *rac*-PO on D-cysteine-modified Au nanoparticles, this is $X = \theta^{rac/D}/|\theta^{rac/D}|$ and the opposite for *rac*-PO on L-cysteine-modified Au nanoparticles, $X = -\theta^{rac/L}/|\theta^{rac/L}|$. The data set of Figure 3 constitutes $N = 20$ measurements, 20 having $X = 1$ and none having $X = -1$, yielding a mean value of $\bar{X} = 1.0$. In the absence of enantiospecific adsorption, the distribution of measurements of X would be characterized by a mean value of $\bar{X} = 0$. Using the statistic $z = \bar{X}/\sqrt{1/N}$, one can reject the hypothesis that there is no enantiospecific adsorption at the 99% level, if $z < -2.58$ or $z > 2.58$.[20] The data set of Figure 2 yields $z = 4.02$, and the data set of Figure 3 yields $z = 4.47$, both rejecting the hypothesis that PO adsorption on D- or L-cysteine modified Au nanoparticles is not enantiospecific.

The use of polarimetry to observe enantiospecific adsorption of chiral compounds from solution onto the surfaces of chiral nanoparticles relies on the fact that the specific rotation of light by the adsorbed species differs from that of the same species in solution. This arises from the enhanced optical rotation imparted by the chiral Au nanoparticles to species adsorbed on their surfaces. As shown in Figure 1, the specific optical rotation constants for (*R*)- and (*S*)-PO in solution are $\alpha^{S}_{sol} = -\alpha^{R}_{sol} = 0.9 \pm 0.06°$/M. When adsorbed on the Au nanoparticles, the magnitude of the specific rotation by (*R*)- and (*S*)-PO clearly

(20) Dixon, W. J.; Massey, F. J. *Introduction to Statistical Analysis*; McGraw-Hill Co.: New York, 1969.

increases. Note that this is observed using the pure enantiomers of (*R*)- and (*S*)-PO adsorbed on unmodified achiral Au nanoparticles and on Au nanoparticles modified by racemic cysteine. It is interesting that the magnitude of the observed enhancement does not appear to depend on whether or not the Au nanoparticles have been modified. This suggests that the enhancement of optical rotation is due to the proximity of the PO to the Au core of the nanoparticle and is not influenced by the details of its interactions with the cysteine modified surface. This observation may be fortuitous, however, because even if the specific optical rotation constant for the adsorbed phase is not influenced by the presence of cysteine on the surface, the partitioning of the PO between solution phase and the adsorbed phase ought to be influenced by the modification of the Au nanoparticles.

The enantiospecific interaction of (*R*)- or (*S*)-PO with D- or L-cys/Au is revealed by the optical rotations in Figure 2. The magnitudes of the optical rotations for the (*R*)-PO/L-cys/Au and (*S*)-PO/D-cys/Au pairs are greater than those of the (*R*)-PO/D-cys/Au and (*S*)-PO/L-cys/Au pairs. This is a true diastereomeric effect. The comparison with the optical rotations for just (*R*)- or (*S*)-PO in solution also reveals the enhanced optical rotation by PO adsorbed on the Au nanoparticles.

The adsorption of the PO onto the Au nanoparticles can be described in the simplest terms using a Langmuir model for adsorption. For adsorption of (*R*)-PO onto the D-cys/Au nanoparticles the concentration of the adsorbed fraction, x^R_{ads}, is given by

$$\frac{x^R_{ads}}{S_0} = \frac{K^R_D \cdot x^R_{sol}}{1 + K^R_D \cdot x^R_{sol}} \qquad (1)$$
$$x^R_{tot} = x^R_{ads} + x^R_{sol}$$

where x^R_{tot} is the total concentration of (*R*)-PO in the solution and x^R_{sol} is the concentration in the solution phase. The quantity K^R_D is the equilibrium binding constant at room temperature for (*R*)-PO adsorption onto the D-cys/Au nanoparticles and S_0 is the concentration of adsorption sites on the Au nanoparticles in the solution. Note that the concentration of binding sites is in the same volumetric units (M) as the concentrations of the PO. Given K^R_D and S_0, one can evaluate x^R_{ads} and x^R_{sol} as functions of x^R_{tot}, the experimentally controlled independent variable.

$$x^R_{sol}(x^R_{tot};K^R_D, S_0) = [(K^R_D x^R_{tot} - 1 - K^R_D S_0) + ((K^R_D x^R_{tot} - 1 - K^R_D S_0)^2 + 4K^R_D x^R_{tot})^{1/2}]/2K^R_D \text{ and } x^R_{ads}(x^R_{tot};K^R_D, S_0) = x^R_{tot} - x^R_{sol} \qquad (2)$$

Similar adsorption isotherms describe all four combinations of (*R*)- or (*S*)-PO in solution with D- or L-cys/Au and they yield similar expressions for the partitioning of PO between the adsorbed and the solution phase.

For adsorption of (*R*)-PO onto the D-cys/Au nanoparticles, the rotations of polarized light are determined by the distribution of (*R*)-PO between the adsorbed and the solution phases and by α^R_{ads} and α^R_{sol}, the specific optical rotations for (*R*)-PO in the adsorbed and the solution phases, respectively. The optical rotation for just (*R*)-PO in solution (without cysteine or Au nanoparticles) is given by

$$\alpha^R(x^R_{tot}) = \alpha^R_{sol} x^R_{sol} \text{ with } x^R_{tot} = x^R_{sol} \qquad (3)$$

A similar expression describes the optical rotation of (*S*)-PO only in solution. The optical rotation for the (*R*)-PO in solution with D-cys/Au nanoparticles is given by

$$\alpha^R_D(x^R_{tot}) = \alpha^R_{sol} x^R_{sol}(x^R_{tot};S_0, K^R_D) + \alpha^R_{ads} x^R_{ads}(x^R_{tot};S_0, K^R_D) \qquad (4)$$

Three similar expressions describe the optical rotation by the other combinations of (*R*)- or (*S*)-PO in solution with D- or L-cys/Au. These six equations for α^R, α^S, α^R_D, α^R_L, α^S_D, and α^S_L describe the six sets of data shown in Figure 2 in terms of five independent parameters: α^S_{sol} ($= -\alpha^R_{sol}$), α^S_{ads} ($= -\alpha^R_{ads}$), K^R_D ($= K^S_L$), K^R_L ($= K^S_D$), and S_0. Simultaneous fitting of all six data sets using these five parameters yields the curves plotted with the data in Figure 2. The values of the five parameters estimated by this procedure are listed in Table 1. The errors in the estimated parameter values have been determined from a sensitivity analysis of the fit and are listed in Table 1.

The fit of the adsorption model to the optical rotation data in Figure 2 is imperfect but does capture the basic trends of the data. These are the nonlinear increase in the optical rotation with increasing PO concentration and the enantiospecificity of the optical rotation. One likely source of error in the fit is our use of a simple Langmuir isotherm to describe the adsorption of PO on the cysteine-modified Au nanoparticles. This is the simplest form of adsorption isotherm and a more complicated isotherm would be needed to better fit the experimental data.

The values of the adsorption constants and optical rotation constants resulting from the fit of the data in Figure 2 are consistent with all other observations made thus far, in this work. The value for the specific optical rotation for (*R*)- or (*S*)-PO in the solution phase is $\alpha^S_{sol} = -\alpha^R_{sol} = 0.9 \pm 0.04°/M$ in exact agreement with the linear fits to the data in Figure 1. The value of $\alpha^S_{ads} = -\alpha^R_{ads} = 2.2 \pm 0.3°/M$ is greater than the lower limit of $1.7 \pm 0.1°/M$ predicted by the slope at [PO] = 0 of the quadratic fit to the data in Figure 1. The concentration of binding sites for PO in solutions containing cys/Au nanoparticles is $S_0 = 0.23 \pm 0.07$ M, which is consistent with the fact that the optical rotation is nonlinear in the PO concentration range below [PO] = 0.5 M. Finally, and most importantly, the values of the adsorption equilibrium constants are $K^R_D = K^S_L = 8.1 \pm 3.1/M$ and $K^R_L = K^S_D = 50 \pm 1/M$ and indicate a significant enantiospecificity for binding of (*R*)- or (*S*)-PO to D- or L-cys/Au. The fact that the uncertainty in the value of K^R_D ($= K^S_L$) is greater than that for K^R_L ($= K^S_D$) is reflective of the fact that the fit of the model to the data for (*R*)-PO/D-cys/Au (or (*S*)-PO/L-cys/Au) is not as good as the fit to the data for (*R*)-PO/L-cys/Au (or (*S*)-PO/D-cys/Au).

The enantiospecific difference in the binding constants for (*R*)- or (*S*)-PO on D- or L-cys/Au, $K^R_D = K^S_L \neq K^S_D = K^R_L$, indicate

Table 1. Adsorption and Optical Rotation Parameters for PO Adsorption onto the Surfaces of Chirally Modified Au Nanoparticles

parameter		value[a]
α^S_{sol}	$-\alpha^R_{sol}$	$0.90 \pm 0.04°/M$
α^S_{ads}	$-\alpha^R_{ads}$	$2.2 \pm 0.3°/M$
K^R_D	K^S_L	$8.1 \pm 3.1°/M$
K^R_L	K^S_D	$50 \pm 1°/M$
S_0		$0.23 \pm 0.07M$

[a] The five parameters, *P*, were determined by fitting the entire data set shown in Figure 2 to the model. Errors are reported as standard deviations, σ_P, determined from a sensitivity analysis of the each parameter to variance in the measured values of the optical rotation at different concentrations, $\{y_i\}$. The variances are defined as $\sigma^2_P = \sum((dP)/(dy))^2 \sigma^2_y$ with $\sigma^2_y = (SSE)/(N - 5)$ where SSE is the sum of the squared errors between the $N = 56$ data points and the fitted model.

that the cys/Au nanoparticles can be used for enantioselective separation of *rac*-PO. The two enantiomers of the PO partition differently and enantiospecifically between the solution phase and adsorbed phase. However, this would not be observable using optical rotation if it were not for the fact that the specific optical rotation by adsorbed PO is significantly greater than that of solution-phase PO. As revealed by the data in Figure 3, addition of *rac*-PO to a solution containing D- or L-cys/Au does indeed result in optical rotation with a magnitude of $\alpha_D^{rac} = -\alpha_L^{rac} = 0.15 \pm 0.01°/M$. Description of the adsorption of (*R*)- and (*S*)-PO from a solution of *rac*-PO onto D- or L-cys/Au is complicated by the fact that the (*R*)- and (*S*)-PO adsorb competitively with one another. However, in the limit of low concentrations, the adsorption isotherm gives the concentrations in the solution phase and the adsorbed phase

$$x_{sol}^{R} = \frac{x_{tot}^{rac}/2}{1 + S_0 K^{R}} \qquad x_{ads}^{R} = \frac{S_0 K^{R} x_{tot}^{rac}/2}{1 + S_0 K^{R}} \tag{5}$$

with similar expressions describing x_{sol}^{S} and x_{ads}^{S}. These yield the following expression for the specific rotation of light by low concentrations of *rac*-PO in the presence of D- or L-cys/Au

$$\alpha_D^{rac} = -\alpha_L^{rac} = \frac{1}{2}\left(\left(\frac{\alpha_{sol} + \alpha_{ads} S_0 K_D^{S}}{1 + S_0 K_D^{S}}\right) - \left(\frac{\alpha_{sol} + \alpha_{ads} S_0 K_D^{R}}{1 + S_0 K_D^{R}}\right)\right) \tag{6}$$

where $\alpha_{sol} = \alpha_{sol}^{S} = -\alpha_{sol}^{R}$ and $\alpha_{ads} = \alpha_{ads}^{S} = -\alpha_{ads}^{R}$. Given the values of the adsorption equilibrium constants and optical rotation parameters found from the data in Figure 2 (in Table 1), this expression predicts that at low concentrations of *rac*-PO, the optical rotation of light in the presence of D- or L-cys/Au will be $\alpha_D^{rac} = -\alpha_L^{rac} = 0.19°/M$, in fairly close agreement with the value of 0.15°/M indicated by the data in Figure 3.

The logic behind the reported demonstration of the enantiospecific interaction of PO with chirally modified Au nanoparticles can be summarized in three steps. First, the data in Figure 1 indicate that there is an enhancement in the optical rotation of light by PO interacting with Au nanoparticles. This enhancement is independent of whether the surfaces of the Au nanoparticles have been modified with cysteine. The data in Figure 2 show enantiospecific optical rotation of (*R*)- or (*S*)-PO interacting with enantiomerically pure D- or L-cys/Au. These data have been interpreted in terms of an adsorption model to yield quantitative estimates of the optical rotation constants of PO in the adsorbed and solution phases and quantitative estimates of the enantiospecific adsorption equilibrium constants for (*R*)- or (*S*)-PO on D- or L-cys/Au. Finally, the adsorption model and adsorption equilibrium constants have then been used to accurately predict the data in Figure 3 showing the optical rotation induced by addition of racemic PO to solutions containing enantiomerically pure D- or L-cys/Au.

The work described herein suggests many interesting avenues for future investigation and potential applications of chiral metallic nanoparticles. One of the possibilities is that metallic nanoparticles might be used to enhance the sensitivity of methods for detection of enantiomeric excess in dilute solutions or for detection of species with low specific optical rotation in solution. There is no doubt that control of nanoparticle size and composition can be used to further enhance this effect and is being explored. A directly related issue is that of the physical origin of the enhancement of optical activity by metallic nanoparticles. Finally, the methods used in this investigation offer a relatively simple approach to quantitative understanding of enantiospecific interactions between chiral probes and chiral metal nanoparticles. This can be used as the basis for understanding the origins of enantioselectivity on chiral surfaces.

Conclusions

The work presented clearly reveals the potential of metal nanoparticles to serve as enantiospecific adsorbents of chiral species. This has been illustrated by study of the interactions of (*R*)-, (*S*)-, or *rac*-PO with Au nanoparticles modified with D-, L-, or *rac*-cys/Au. The necessary characteristic of chiral adsorbate-nanoparticle systems that leads to enantiospecific adsorption and the potential for separation of racemic mixtures is the fact that the adsorption equilibrium constants are enantiospecific, $K_D^R = K_L^S \neq K_D^S = K_L^R$. In the case of PO adsorption on cys/Au nanoparticles, the values of these equilibrium constants are significantly enantiospecific; $K_D^R = K_L^S = 8.1 \pm 3.1/M$ and $K_L^R = K_D^S = 50 \pm 1/M$. Observation of enantiospecific interactions using polarimetry relies on the fact that adsorption of chiral species on the Au nanoparticles results in enhanced specific optical rotation constants. In the case of PO in solution and adsorbed on Au nanoparticles, these are $\alpha_{sol}^S = -\alpha_{sol}^R = 0.9 \pm 0.04°/M$ and $\alpha_{ads}^S = -\alpha_{ads}^R = 2.2 \pm 0.3°/M$.

Acknowledgment. A.J.G. acknowledges support from the DOE under grant no. DE-FG02-03ER15472. M.A.B. acknowledges support from a CMU SURG grant.

JA908219H